ORIGINAL PAPER

N-acetylglucosamine-6-phosphate deacetylase (NagA) of *Listeria monocytogenes* EGD, an essential enzyme for the metabolism and recycling of amino sugars

Magdalena Popowska · Magdalena Osińska · Magdalena Rzeczkowska

Abstract The main aim of our study was to determine the physiological function of NagA enzyme in the *Listeria monocytogenes* cell. The primary structure of the murein of *L. monocytogenes* is very similar to that of *Escherichia coli*, the main differences being amidation of diamino-pimelic acid and partial de-*N*-acetylation of glucosamine residues. NagA is needed for the deacetylation of *N*-acetyl-glucosamine-6 phosphate to glucosamine-6 phosphate and acetate. Analysis of the *L. monocytogenes* genome reveals the presence of two proteins with NagA domain, Lmo0956 and Lmo2108, which are cytoplasmic putative proteins. We introduced independent mutations into the structural genes for the two proteins. In-depth characterization of one of these mutants, MN1, deficient in protein Lmo0956 revealed strikingly altered cell morphology, strongly reduced cell wall murein content and decreased sensitivity to cell wall hydrolase, mutanolysin and peptide antibiotic, colistin. The gene products of operon 150, consisting of three genes: *lmo0956*, *lmo0957,* and *lmo0958*, are necessary for the cytosolic steps of the amino-sugar-recycling pathway. The cytoplasmic de-*N*-acetylase Lmo0956 of *L. monocytogenes* is required for cell wall peptidoglycan and teichoic acid biosynthesis and is also essential for bacterial cell growth, cell division, and sensitivity to cell wall hydrolases and peptide antibiotics.

Keywords *Listeria monocytogenes* ·
N-acetylglucosamine-6-phosphate deacetylase ·
Amino-sugar catabolism · Peptidoglycan ·
Teichoic acid · Mutanolysin · Colistin

Communicated by Wolfgang Buckel.

M. Popowska (✉) · M. Osińska · M. Rzeczkowska
Department of Applied Microbiology, Institute of Microbiology,
Faculty of Biology, University of Warsaw, Miecznikowa 1,
02-096 Warsaw, Poland
e-mail: magdapop@biol.uw.edu.pl

Introduction

Listeria monocytogenes is a gram-positive bacterium widespread in diverse environments such as waters, soil, rotting parts of plants, animal feces and wastewaters, various food products, humans and animals. *Listeria monocytogenes* is pathogenic for people and animals and is the etiological factor of listeriosis, which mainly affects immunocompromised individuals, pregnant women and newborns. Infection is usually related to the ingestion of food products contaminated with the bacterium, and for this reason, listeriosis is considered a food-borne disease (Joseph and Goebel 2007; Schlech 2000; Scortti et al. 2007; Seveau et al. 2007). The main symptoms of infection are meningoencephalitis, bacteremia and perinatal listeriosis, resulting in death in about 30% of cases. *Listeria monocytogenes* can also cause endocarditis, hepatitis, pleuritis, localized abscesses (e.g. in the brain) as well as muscular, skeletal and skin infections (Ramaswamy et al. 2007).

The primary structure of the murein (syn. peptidoglycan, PG) of *L. monocytogenes* resembles that of *Escherichia coli*. It is composed of glycan chains in which alternating *N*-acetylglucosamine (GlcNAc) and *N*-acetylmuramic acid (MurNAc) are β-1,4 bound. A pentapeptide is linked to MurNAc, and the glycan chains are cross-linked by 4 → 3

linkages between the D-Ala residue of one lateral peptide and the *m*-Dap (acid-*meso*-diaminopimelic) residue of another (Bouhss et al. 2007; Vollmer 2007; Vollmer et al. 2008). Also 3 → 3 cross-links between two adjacent m-Dap residues, like in *E. coli*, are present. The average cross-linkage of *L. monocytogenes* PG is in the ∼65% range. Partial deacetylation of GlcNAc residues (approx. 50%) by PgdA enzyme is another characteristic of *Listeria* peptidoglycan (Boneca et al. 2007; Popowska et al. 2009).

Listeria monocytogenes contains two different polyanionic polymers decorating the cell wall: the teichoic acids (TAs), which are covalently bound to the peptidoglycan, and the lipoteichoic acids (LTAs), which are anchored in the plasma membrane by a diacylglycerolipid. These polymers play important functions in metal cation homeostasis, anchoring of surface proteins, and transport of ions, nutrients, and proteins and are the main determinants of surface immunogenicity, conferring most of the basis of serotype diversity in *L. monocytogenes* (Weidenmaier and Peschel 2008). Of note, D-Ala esterification of TAs and LTAs is important for *L. monocytogenes* pathogenicity.

In *B. subtilis*, the construction and characterization of knockout and conditional mutants in several genes of the TA biosynthetic pathway have established that TA is essential for cell viability (Soldo et al. 2002a, b; Wecke et al. 1997). It is known that different species have different requirements for TA, suggesting that the polymer may display different functions. As major constituents of the surfaces of gram-positive bacteria, TAs have an impact on a number of important biological processes, such as autolysis (Bouhss et al. 2007), binding of cations and surface-associated proteins (Hughes et al. 1973; Jonquieres et al. 1999), adhesion (Abachin et al. 2002; Vollmer and Tomasz 2000; Weidenmaier and Peschel 2008), biofilm formation (Gross et al. 2001), coaggregation (Clemans et al. 1999), resistance to antimicrobial agents such as cationic peptide (Kovacs et al. 2006; Peschel et al. 1999, 2000), protein secretion (Nouaille et al. 2004), acid tolerance (Boyd et al. 2000), stimulation of immune response (Gross et al. 2001; Morath et al. 2001), and virulence (Abachin et al. 2002; Collins et al. 2002; Dubail et al. 2006; Weidenmaier et al. 2004).

The first committed step in the biosynthetic pathway to the amino-sugar precursors required for cell wall peptidoglycan and teichoic acid (TA) biosynthesis in *L. monocytogenes* is the deacetylation of *N*-acetyl-glucosamine-6 phosphate (GlcNAc-6-P) to glucosamine-6 phosphate (GlcN-6-P) and acetate (Park and Uehara 2008) (Fig. 1). Deacetylation of *N*-acetylglucosamine is also important in lipopolysaccharide synthesis and cell wall recycling. GlcN-6-P is a normal intermediate in the pathway for the synthesis of UDP-GlcNAc. Alternatively, GlcN-6-P can be converted to fructose-6-P by NagB (*lmo0957*). In gram-
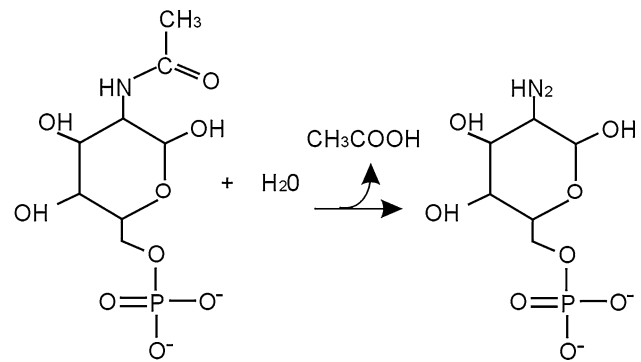

Fig. 1 The chemical reaction catalyzed by NagA, a *N*-acetylglucosamine-6-phosphate de-*N*-acetylase (**N**)

negative bacteria like *E. coli* this step is also important in lipopolysaccharide synthesis and cell wall amino-sugar recycling: (GlcN-6-P and 1,6-anhydro-*N*-acetyl-muramic acid-anhMurNAc). The enzyme responsible for this reaction is *N*-acetyl-glucosamine-6 phosphate deacetylase, NagA (EC 3.5.1.25) (Barnhart et al. 2006; Park 2001; Jaeger and Mayer 2007) with conserved domain cd00854 representative of the structural superfamily of metal-dependent hydrolases, involving a binuclear Fe catalytic center. The *L. monocytogenes* biosynthetic pathway to amino-sugar-nucleotides with participation of a NagA-type enzyme is very similar to that proposed by Vincent et al. (2004) for *B. subtilis* (Vincent et al. 2004). As the result of analysis of the *L. monocytogenes* genome (Glaser et al. 2001) (BLAST—similar conserved domain architecture) analogous proteins catalyzing each step of the amino-sugar metabolism pathway in *L. monocytogenes* were found (this work, Fig. 2). An *N*-acetylglucosamine-6-P deacetylase is an essential enzyme for the metabolism of amino sugars and for recycling GlcNAc and anhMurNAc. As indicated in Fig. 2, conversion of GlcNAc-6-P to UDP-GlcNAc requires that it first be deacetylated by NagA and then converted to GlcN-1-P by GlmM, followed by reacetylation and reaction with UTP by GlmU to form UDP-GlcNAc. Alternatively, GlcN-6-P can be converted to fructose-6-P by NagB. As indicated, the reverse reaction to Glc-N-6-P is catalyzed by GlmS.

Analysis of the *L. monocytogenes* genome reveals the presence of 2 proteins with NagA domain, Lmo0956 and Lmo2108, that are likely to be cytoplasmic, as opposed to previously identified Lmo0415 (PgdA) (Boneca et al. 2007; Popowska et al. 2009). We present here the results of mutating *L. monocytogenes* gene *lmo0956*. We expected that the construction of a strain deficient in *N*-acetyl-glucosamine-6 phosphate deacetylase would permit determining the physiological role of this enzyme in vivo and have found that the examined protein is essential for bacterial cell growth, cell division, and sensitivity to a cell
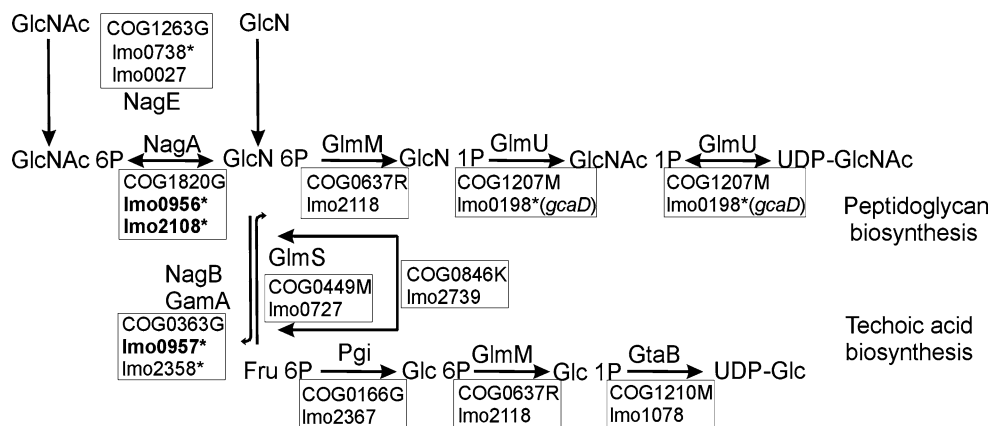
Fig. 2 Proposed pathways of recycling and amino-sugar metabolism in *L. monocytogenes* based on those in *B. subtilis*, including the proteins predicted to be involved in this process—a schematic representation of *L. monocytogenes* cytoplasmic proteins potentially involved in amino-sugar metabolism. Abbreviations: *Fru* fructose, *Glu* glucose. Gene products: NagA, GlcN-6-P de-*N*-acetylase; NagB, GlcN-6-P isomerase; GlmS, L-glutamate-D-fructose-6-P amido-transferase; GlmM, phosphoglucomutase; GlmU, UDP-GlcNAc pyrophosphorylase; Pgi, Glc-6-P isomerase; GtaB, UTP-Glc_1-P uridyltransferase; NagP, GamP, phosphotransferases. The symbol (*asterisk*) indicates genes which are organized in an operon structure (according to Toledo-Arana et al. 2009)

wall hydrolase, mutanolysin and peptide antibiotic, colistin.

Materials and methods

Bacterial strains, plasmids, primers, and growth conditions

Listeria monocytogenes strains were grown in Tryptic Soy Broth containing yeast extract (TSYEB; BTL) at 37°C with constant shaking (150 r.p.m.) unless otherwise stated, or on TSYEA plates (1%, w/v agar). In the case of *L. monocytogenes* mutant strains, the growth medium was supplemented with 0.1% agar or 20% sucrose or one of the following sugars: glucosamine, glucose-6-phosphate, and *N*-acetylglucosamine in concentration 10, 20, and 50 mg/ml. *Escherichia coli* DH5α were grown in Luria–Bertani broth (LBL or LB agar 1%, w/v; BTL) at 37°C. Erythromycin (Sigma; 300 μg/ml for *E. coli* and 1.5 μg/ml for *L. monocytogenes*) were added to broth or agar as needed. When necessary, 0.1 mM IPTG (isopropyl-*β*-D-thiogalactopyranoside) and X-Gal (5-bromo-4-chloro-3-indolyl-*β*-D-galactopyranoside) (20 μg/ml) were spread on agar plates 30 min prior to plating. Bacterial strains, plasmids, and primers used in this study are shown in Tables 1 and 2.

Table 1 Bacterial strains and plasmids used in this study

Strain	Relevant genotype or phenotype	Reference or source
E. coli TOP 10	F⁻ *mcrA* Δ(*mrr-had*RMS-*mcr*BC) φ80*lacZ* ΔM15 Δ*lacX*74 *deo*R *rec*A1 *ara*D139 Δ(*araA-leu*)7697 *galU galK rpsL endA1 nupG* (Invitrogen)	Novagen
E. coli DH5α	F⁻ Φ80d *lacZ*M15 (*lacZYA-org*F) U169 *deo*R *rec*A1 *end*A1 *hsd*R17 *pho*A *sup*E44	Novagen
	λ⁻*thi*-1 *gyr*A96 *rel*A1	
L. monocytogenes EGD	Wild type	Institut Pasteur (France)
L. monocytogenes MN1	*nagA*(*lmo0956*) mutant	This study
L. monocytogenes MN2	*Lmo2108* mutant	This study
Plasmids		
PGEM-T Easy	Ap^r; 3.0 kb cloning vector with T overhangs	Promega
pAUL-A	Em^r; 9.2 kb vector plasmid for insertional mutagenesis; thermosensitive replicon from pE194	[30]
pAUL-A::*lmo0956*	Em^r; 9.7 kb; 0.748 kb fragment of gene *lmo0956*, cloned into the *Eco*RI (MCS) site in pAULA	This study
pAUL-A::*lmo2108*	Em^r; 9.7 kb; 0.703 kb fragment of gene *lmo2108*, cloned into the *Eco*RI (MCS) site in pAULA	This study

MCS multiple cloning site

Table 2 Primers used and constructed in this study

Primers	Sequence
FpAUL-A	CCCAGTCACGACGTTGTAAAACG
RpAUL-A	AGCGGATAACAATTTCACACAGG
F0955	GACGCAGAACGCATGGTAGA
R0955	TCCATTAGATCATCGAAGGATTGAG
F0956	GCAGATCCAGAAGCACTTAG
R0956	CTTCTACCGGCATCCAGTAA
F0957	GGCATTACATCAGGCGAAGT
R0957	GCCTCGTTGTCAAGAATCAC
F0958	GGCACTTCTATTCCAGCTGA
R0958	GTCGACCGTCTTCTAACGTT
F2107	AGTGGAGGAACTGAAGCTGC
R2107	GCCTGATAATACGCGCGATT
F2108	CTGTATCTATGGCTTGTGCG
R2108	CGTCACGGTACTTGAAGCTA
F2109	GTGATGGGACTATATTACTTAGG
R2109	TGAGTTGCTTAGGATGAATGTATT

Fluorescence microscopy of DAPI stained cells

Harvested cells were washed once with PBS, and then resuspended in PBS containing 0.1% Triton X (to induce perforation of the cells membrane and increase its permeability) and incubated for 10 min on ice. The cells were harvested again and resuspended at 5,000 cells/µl in 4% PBS buffered paraformaldehyde solution containing 10 µg/ml 4′6-diamidino-2-phenylindole (DAPI, Sigma). Ten microliters of this suspension were placed on a glass slide and covered with a coverslip. The morphology of the cells was observed using a fluorescence microscope (Olympus BH Series) at excitation wavelength 350 nm (Porter and Feig 1980).

Preparations for electron microscopy

Bacterial cells from log phase of culture were collected on Millipore HA filter. The cells were fixed for 30 min in 4% paraformaldehyde, washed 3 times in PBS buffer, pH 7.4, and then dehydrated using a series of 15 min incubations in 25, 50, 75, and 100% ethanol. The preparations were coated with gold and viewed in LEO 1430VP scanning microscope. Bacterial cells for observation under transmission electron microscope were prepared by using a thin-sectioning procedure previously described by Matias and Beveridge (2006).

Measurement of bacterial cell length and thickness of bacterial cell wall

In every case, 120 bacterial cells or thin sections were selected on the micrographs and measured using the

ImageJ program developed at the National Institutes of Health (http://imagej.nih.gov/ij/index.html). The magnifications of the cells in the micrographs take the bar into consideration.

DNA isolation and manipulations

Standard protocols were used for recombinant DNA techniques (Sambrook and Russel 2001). DNA fragment used in the cloning procedures and PCR products were isolated from agarose gels with the DNA Gel-Out extraction kit (A&A Biotechnology) according to the manufacturer's instructions. Plasmid DNA from *E. coli* was isolated and purified with the Plasmid Miniprep Plus kit (A&A Biotechnology). The procedures for the isolation of plasmid and chromosomal DNA from *L. monocytogenes* were performed as previously described (Popowska and Markiewicz 2006), starting with digestion of the bacterial cell wall in 5–10 mg/ml lysozyme-containing GTE buffer for 1 h at 37°C.

Inactivation of genes lmo0956 and lmo1208

The genes encoding the protein with *N*-acetyl-glucosamine-6 phosphate deacetylase activity were inactivated by insertional duplication mutagenesis as described before (Machata et al. 2005; Popowska and Markiewicz 2006; Popowska et al. 2009). The Internal (a) 748 bp fragment of gene *lmo0956*, or (b) 703 bp fragment of gene *lmo2108*, was cloned into vector pAUL-A (Em^r) (Schäferkordt and Chakraborty 1995). The fragments were amplified from chromosomal DNA of strain EGD by PCR using the respective starters: F0956 and R0956 or F2108 and R2108 (Table 2). The PCR reaction was performed in a total volume of 100 µl with 40 ng of template DNA, 50 pmol of primers, 0.1 mM dNTP, and 2 units of Taq polymerase (Fermentas) using the fallowing conditions: 94°C for 5 min, 30 cycles of 94°C for 30 s, 55°C or 60°C for 30 s, 72°C for 1 min, and one final extension step at 72°C for 5 min. The amplified fragments, after purification (NucleoSpin; Macherey–Nagel), were then initially cloned into vector pGEM-T Easy (Promega). In effect, two recombined plasmids pGEM1 and pGEM2 (carrying fragments of genes *lmo09566* and *lmo2108*, respectively) were obtained. Plasmids pGEM1 and pGEM2 were digested with *EcoRI*, and the inserts isolated from agarose gel, after purification (NucleoSpin; Macherey–Nagel), were ligated into pAUL-A (pre-digested with *EcoRI*). The resulting vectors p0956 and p2108 were transformed into *E. coli* DH5α with selection for erythromycin resistance. Finally, the plasmids were isolated (NucleoSpin; Macherey–Nagel) and the correctness of the constructs was confirmed by restriction analysis. The plasmids p0956 and

p2108 were introduced into *L. monocytogenes* cells by electroporation at 30°C. Since *L. monocytogenes* contains a thick cell wall containing teichoic acids linked to murein, electrocompetent cells were prepared in the presence of penicillin (Park and Stewart 1990). Following electrotransformation, colonies of *L. monocytogenes* EGD resistant to erythromycin 1 μg/ml (plasmid marker) were selected. Transformants were grown in TSYEB broth containing 1 μg erythromycin per ml at 30°C for 12 h. The culture was diluted 1/100 into fresh TSB containing erythromycin (1 μg/ml) at 42°C. Overnight cultures of the obtained clones were spread on plates containing erythromycin and incubated at 42°C for 12 h. In both cases, several transformants were picked, and the correct incorporation of the plasmid into a specific site on the chromosome was confirmed by PCR analysis and by hybridization (data not shown).

The obtained insertion mutants (Em^r) EGD/pAUL-A::*lmo0956* were designated: MN1 and EGD/pAUL-A::*lmo2108* MN2. These mutants were used in an analysis of the role of proteins Lmo0956 and Lmo2108 in cell physiology. The mutants were able to grow in 1 μg/ml erythromycin. However, because the growth rate was reduced, erythromycin was included only in the pre-culture and not in the culture used for the experiments in order to have growth conditions similar to that of the parental strain.

RT-PCR

RNA was isolated as described elsewhere (Sambrook and Russel 2001). Isolated RNA, in DEPC-treated water, was incubated with buffer for DNase I and 5U of DNase I (RNase free) at room temperature for 15 min. To stop the reaction, EDTA made up in DEPC-treated water was added to final concentration 1 mM and incubated for 10 min at 60°C. cDNA was synthesized from 2 μl of RNA using RevertAid^{TM} H Minus First Strand cDNA Synthesis Kit (Fermentas) using sequence-specific primer. Aliquots (2 μl) of the resulting cDNA were amplified by PCR with specific primers (Table 2) and Taq polymerase and samples were taken and run on agarose gels. In the case of mutant MN1, the template used to demonstrate the presence of transcript for the gene upstream—*lmo0955*—was cDNA formed with the use of RTB1 primer, for the genes downstream—*lmo0957* and *lmo0958*—cDNA formed with the use of RTA1 primer. For mutant MP2, the template used to demonstrate the presence of the transcript for the gene upstream—*lmo2107*—was cDNA formed using RTB2 primer, for the gene downstream—*lmo2709*—cDNA formed using RTA2 primer (Fig. 6). Reverse transcriptase-PCR products were electrophoresed in 2% agarose gel.

Cell wall isolation

Listeria monocytogenes cells were harvested by centrifugation and resuspended in 1/40 of the original culture volume of ice-cold saline. Glass beads (diameter 150–215 μm; Sigma) were added (1 g per 1 ml cell suspension) and then 1 min bursts of ultrasound waves were employed in VCX-600 ultrasonicator (Sonics and Materials, USA) at amplitude 20%. The crude cell wall preparation was sedimented by centrifugation in a Beckman centrifuge (25 min, 100,000g at 4°C). The cell pellet was suspended in ice-cold water and added dropwise to the same amount of boiling 8% SDS with vigorous stirring throughout. The samples were kept boiling for 30 min and then allowed to stand at room temperature overnight. Sacculi were collected by centrifugation (30 min, 150,000g at 22°C) and the pellet was washed with room temperature water five times (a). After each wash, the pellet was resuspended homogeneously and centrifuged in the same conditions (Glauner 1988).

Cell wall purification

The SDS-free pellet was resuspended in 49% (v/v) hydrofluoric acid and incubated for 40 h with stirring in an ice bath to remove teichoic acid. The murein was recovered by centrifugation and washed repeatedly in water as above to remove all hydrofluoric acid (b). The murein was resuspended in 10 mM Tris–HCl buffer (pH 7.0) and weighed again, then treated with α-amylase (100 μg/ml) for 2 h at 37°C, then pre-digested pronase E (200 μg/ml) was added and the incubation was continued for 90 min at 60°C. Finally, the sample was mixed with 8% SDS and incubated for 15 min at 100°C. SDS was removed by washing in distilled water and centrifugation as described above (c). *N*-acetylation of murein was performed with acetic anhydride in the presence of NaHCO$_3$ as described by Hayashi et al. (1973) (d). After each step from (a) to (d) the murein (pellet) was resuspended homogeneously in the same volume of water or buffer and was weighed.

Murein and muropeptide concentrations were calculated from their diamino acid content. Samples were hydrolyzed in 6 N HCl (12 h, 105°C), vacuum dried, and resuspended in an appropriate volume of distilled water. *N*-acetylated murein prepared from wild-type and the mutant was analyzed by HPLC after digestion with the muramidase mutanolysin M1 (Sigma-Aldrich). The concentration of murein was 1 mg/ml and that of the muropeptides was in the range 0.2–0.5 mg/ml.

High-performance liquid chromatography (HPLC)

N-acetylated murein prepared from the parental strain and mutants was analyzed after digestion with the muramidase

mutanolysin M1 (Sigma-Aldrich) by HPLC using the conditions described in detail by Glauner (1988) on Hypersil RP18 column (250 mm × 4 mm, particle size 3 μm diameter; Teknochroma). The elution buffers were 50 mM sodium phosphate, pH 4.35 (A) and 15% methanol in 75 mM sodium phosphate, pH 4.95 (B). Elution conditions were 7 min isocratic elution in buffer A, 115 of linear gradient to 100% buffer B, and 28 min of isocratic elution in buffer B. The flow rate was 0.5 ml/min and the column temperature was 55°C. The separated muropeptides were detected by UV-absorption at 205 nm.

Estimation of cell wall phosphate

Cell walls were prepared essentially as above (cell wall isolation) and the phosphate concentration was determined according to the method of Chen et al. (1956) using the Phosphate Cell Test (Merck) (Ames 1966). In sulfuric solution, orthophosphate ions react with molybdate ions to form molybdophosphoric acid. Ascorbic acid reduces this to phosphomolybdenum blue (PMB) that is determined photometrically. The method is analogous to EPA 365.2 + 3, US Standard Methods 4500-P E, and ISO 6878.

Determination of susceptibility to cell wall hydrolase

Examination of the susceptibility of the mutant to lysis after incubation with mutanolysin was used to assess the integrity of the cell wall. Bacterial cultures (EGD and MN1) were grown in TSYEB supplemented with 20% sucrose and then adjusted to a final OD_{600} of 0.8, collected by centrifugation, and resuspended in lysis buffer (50 mM NaH_2PO_4 buffer at pH 6.8) containing mutanolysin (Sigma) at a final concentration of 20 μg/ml. Suspensions were incubated at 37°C, and lysis monitored spectrophotometrically (Novaspec II spectrophotometer LKB-13; Pharmacia) by determining the decrease in the OD_{600} of the sample over time (at 15-min intervals for 90 min), as previously described (Piuri et al. 2005; Popowska et al. 2009).

Antibiotic sensitivity assays

The susceptibility of the *L. monocytogenes* strains to the antimicrobial peptide colistin sulfate (cyclic polypeptide antibiotic from *Bacillus colistinus*), β-lactam: imipenem; tetracycline; glycopeptide: vancomycin; third-generation cephalosporin: ceftriaxone; and aminoglycoside: gentamicin (Oxoid) was determined on Mueller–Hinton solid medium plates by the standard EUCAST disk diffusion method (European Committee on Antimicrobial Susceptibility 2009).

Results and discussion

Genomic analysis of genes encoding murein deacetylase Lmo0956 and Lmo2108

Studies *in silico* revealed the presence in the *Listeria monocytogenes* EGD genome of two genes coding for potential cytoplasmic deacetylases (Lmo0956 and Lmo2108). The deduced sequences of *lmo0956* (GenBank:NP_464481) and *lmo2108* (GenBank:NP_465632) are of the same length and both are 1,134 bp long and consist of 377 amino acids. A comparison of the sequences of proteins Lmo0956 and Lmo2108 revealed homology (33% identity, 54% similarity), as shown in Table 3. These two proteins exhibit the highest identity to the GlcNAc-6-P deacetylases, for example, from *B. subtilis* and *E. coli*. The greatest similarity is in the strongly conserved part primary sequence of the compared proteins (Supplementary Fig. S1).

Gene *lmo0956* codes for a protein with mass 41,414 Da and isolectric point pI = 5.43, whereas the mass of Lmo2108 is 40,915 Da and its pI = 5.79. *In silico* analysis revealed the presence in both proteins of an identical domain, 100% in the case of Lmo0956 with *E*-value— 5.26e − 125 and 99.7% in the case of Lmo2108 with *E*-value—1.84e − 118, to the characteristic and highly conserved NagA domain (Cd00854) (Vincent et al. 2004), which is a *N*-acetyl-D-glucosamine-6-phosphate deacetylase. This enzyme type is involved in *N*-acetylglucosamine metabolic processes (Fig. 2) (chemical reactions and

Table 3 Comparison of *L. monocytogenes* NagA proteins with other NagAs

	Identity/similarity [%]	
	Lmo0956 *L. monocytogenes* EGD GenBank:NP_464481 (377aa)	Lmo2108 *L. monocytogenes* EGD GenBank:NP_465632 (377aa)
NagA *B. subtilis* 168 GenBank:CAB15506 (396aa)	40/55	36/53
NagA *E. coli* k12 GenBank:NP_415203 (382aa)	31/50	35/54
NagA *T. maritima* GenBank:AAD35896 (364aa)	36/53	35/58
Lmo0956 *L. monocytogenes* EGD GenBank:NP_464481 (377aa)	100/100	33/54

pathways involving *N*-acetylglucosamine). It thus seems plausible that the products of genes *lmo0956* and *lmo2108* carry out the functions of *N*-acetylglucosamine deacetylases in *L. monocytogenes* EGD cells.

The construction of a model of the conserved domain of Lmo0956 protein (modeled residue range: 2–375 from 377 residues) using the server Swiss Model (http://swissmodel.expasy.org) (Schwede et al. 2003) demonstrates its significant similarity to other proteins of this type belonging to the NagA family (Fig. 3). The genome localization of *lmo0956* reveals genes probably coding for proteins involved in amino-sugar metabolism. This region, consisting of three genes: *lmo0956*, *lmo0957*, and *lmo0958*, was identified as operon 150 by Toledo-Arana et al. (2009). Lmo0957 codes for a protein similar to glucosamine-6-phosphate isomerase—NagB (EC 5.3.1.10). The two genes *lmo0956* and *lmo0957* are certainly regulated by a transcription regulator—*lmo0958*, similar to the GntR family. The next gene, lmo2108, is located in a genome region in which genes participating in mannose metabolism connected with fructose metabolism can be found. This region, consisting of three genes: lmo2107, lmo2108, and lmo2109, was identified as operon 384 (Toledo-Arana et al. 2009). Gene *lmo2109* encodes an alpha/beta hydrolase fold and is located upstream of gene lmo2110, which codes an enzyme similar to mannose 6-phosphate isomerase (EC 5.3.1.8). Expression of *lmo2108* and possibly the other collocated genes is regulated by *lmo2107*, a transcriptional regulator similar to the DeoR family. The possible enzymatic activity and potential function the above proteins are presented in Supplementary Table S1. The same genes and operons were found in the genome of other bacteria, e.g. *E. coli*, *B. subtilis*, *Caulobacter crescentus*, *Salmonella enterica* (Becker et al. 2006; Peri et al. 1990; Vincent et al. 2004). Analysis of the gene order in the NagA cluster indicates that *nagA* exists in an operon nagE-BACD only in few members of the proteobacteria-γ group. In other bacteria, *nagA* can exist in a shorter operon confirming that the operon is unstable in long-term evolution. This gene has also survived strong selection, indicating a conserved functional role in evolution. Sequence analysis provides a basis for the evolution of distinct metal-binding properties within prokaryotic sequences (Arunkumar and Manoj 2010).

The NagA enzyme is included among proteins associated with peptidoglycan (PG) recycling, a process in which the products of turnover are normally reutilized by the cell. The loss of PG by gram-positive bacilli such as *Bacillus subtilis* (Doyle et al. 1988) is about 30% per generation. PG recycling involves several processes: recycling of murein tripeptide, PG amino acids, and PG amino sugars. *Listeria monocytogenes* breaks down about 30–50% of its cell wall PG each generation (Doyle et al. 1982; Szydłowska and Markiewicz 1997). This process has been termed turnover and is defined as an enzymatic process that leads to the excision of fragments from preexisting insoluble wall material. Recycling, in turn, involves the uptake of part of the products from murein turnover back into the cell cytoplasm, after which these molecules are again incorporated into the structure of the murein sacculus. A cell can take up the peptide moieties alone, after they are removed from the muropeptides by amidases, or as whole muropeptides. In the cytoplasm these products are further processed enzymatically prior to being incorporated into murein precursors. In view of the presence of the conserved domain and high degree of identity with analogous proteins of *B. subtilis* (Vincent et al. 2004), it seems that proteins Lmo0956 and Lmo2108 are involved in the deacetylation of muropeptides that have been taken up into the bacterial cell. Taking into account the cytoplasmic location of these proteins in *L. monocytogenes* EGD cells and the presence of the characteristic conserved domain, it seems that the potential function of these enzymes could be participation in the recycling of the cell wall murein as well as indirectly also in the synthesis of this macromolecule and of TAs.
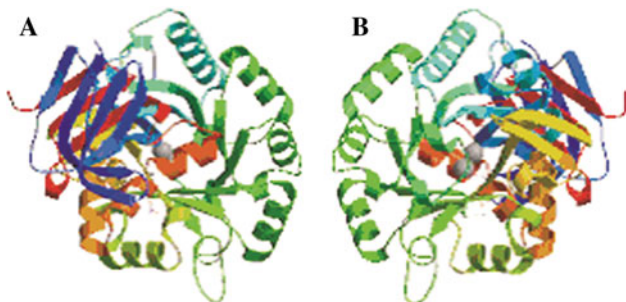
Functional genetic analysis of lmo0956 and lm2108

In order to confirm the suggested activity and participation of operons 150 and 384 in amino-sugar metabolism, mutations were introduced into genes *lmo0956* and *lmo2108* using the thermosensitive vector pAUL-A. The obtained mutants were designated MN1 and MN2, respectively. The site-specific insertion of plasmid into the chromosome was confirmed by PCR and hybridization (results not shown). All attempts to obtain in-frame deletion mutants of these two genes failed, although we applied every well-established method. Similar problems were

Fig. 3 Model of the protein Lmo0956 generated with the use of Swiss Model server (http://swissmodel.expasy.org). Modeled residue range: (**a**) 3 to 375 from 377 residues, based on template 2vhlA (2.05 Å), (**b**) 5 to 363 from 377 residues, based on template 2vhlB (2.05 Å)

described by Mertins et al. (2007) with obtaining in-frame deletion mutants of genes involved in carbon catabolite repression (CCR control system). Complementation of the mutants with the intact gene expressed from plasmid also met with failure, because of the observed chaining phenotypes of the mutants. The method of choice for introducing genetic constructs, such as plasmids, into *Listeria* cells is electroporation. However, all electroporation attempts under different experimental conditions used resulted in complete lysis of the mutant cells. Attempts to obtain deletion mutants were also unsuccessful. This in all probability was due to the fact that the frequency with which a deletion mutant can be selected from a wild-type phenotype pool depends on the physiological fitness of the mutant. Failure in obtaining deletion mutants or mutants with complementary gene on plasmid was due to changes in the structure and thickness of the cell wall of the mutants compared to the wild-type, which was also reflected in their altered morphology. Transcription analysis in RT-PCR reaction using MN1 or MN2 generated cDNA isolated from bacterial cells in logarithmic or stationary phase of growth and using specific primer pairs (Table 2) confirmed the Toledo-Arana et al. (2009) transcription analysis showing that the studied genes are clustered in an operon. As a positive control, analogous PCR reactions were performed using cDNA generated from EGD. The formation of visibly smaller amount of transcript from genes lmo0957 and lmo2109 located downstream of mutated genes *lmo0956* and *lmo2108* from cDNA matrix from the log phase of growth was observed. In the case of cDNA isolated from the stationary phase of growth, the amounts of transcripts from all mentioned genes were similar. Even if a weak polar effect of insertion into genes *lmo0956* and *lmo2108* for downstream genes *(lmo0957* and *lmo2109)* occurs, it can be excluded because the studied genes are located in operons. The achieved results are in accordance with the sequence prediction, which reveals the presence of transcriptional terminators downstream of *lmo0958* and *lmo2109* (Fig. 4). The reactions resulted in products of equal intensity, confirming the formation of transcripts for upstream genes (lmo0955 in the case of mutant MN1 and also for *lmo2107* in the case of mutant MN2) (data not
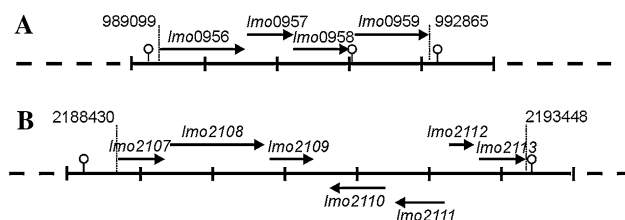
shown). All PCR amplifications were performed according to the scheme presented in Supplementary Fig. S2.

Characterization of cell morphology

When transferred from solid medium to TSYEB the cells of mutants MN1 and MN2 were observed to burst shortly after the beginning of incubation (40–60 min), which coincides with the division time. These observations suggest that the cells of the mutants are not able to survive under the physiological conditions used for the growth of wild-type *L. monocytogenes* EGD. The mutants were able to grow when their growth medium was supplemented with 0.1% agar or 20% sucrose.

The cells of EGD, MN1, and MN2 were also examined by light and fluorescence microscopy when the cultures were in logarithmic and stationary phase of growth (OD_{600} of 0.6 or 2.0). Microscopic observations of 24 h cultures of the mutants in liquid medium revealed striking changes in cell morphology. A large part of the cells formed long chains composed of cells that did not separate following division, with fully formed septum (Supplementary Fig. S3). Older, 48 h, cultures consisted mainly of single cells or cells joined into short chains. Cells of the mutants also grew in the form of long chains on solid medium. The observed changes in cell morphology were more spectacular in the case of MN1; therefore, for further analysis, mutant MN1 was selected. Mutant MN2 (impaired in lmo2108) will be characterized in the future. Experiments with glucosamine, glucose-6-phosphate, or *N*-acetylglucosamine (in the range 1–50 mg/ml) added to the MN1 culture did not reverse the changes in the cell morphology of the mutants, though we expected the wild phenotype to be restored after supplementing the growth medium with the missing sugar. Scanning microscopic observations of these cultures and the control cultures in logarithmic phase showed the presence of long chains, composed of 5–8 cells (Fig. 5a).

These results point to disturbed cell growth and division. The shortening of the cells with prolonged time of incubation of the culture may indicate that the functions of the inactivated enzyme may be taken over by the second, homologous enzyme.

The morphology of mutant MN1 was compared to that of EGD by scanning and transmission electron microscopy. The cultures of both strains that were used to prepare microscope slides were grown under the same conditions in the presence of osmoprotectants. In thin sections (Fig. 6a–d), wild-type bacteria presented the typical morphology of dividing bacteria with formation of septum, normal cell wall thickness, and normal bacterial size (Table 4).

Images obtained from transmission electron microscopy showed that many MN1 cells were apparently arrested during cell division (Fig. 6g–l). Other cells were observed

Fig. 4 Genetic maps of fragments of *L. monocytogenes* EGD genome including Lmo0956 (**a**) and lmo2108 (**b**) genes. Open reading frames and direction of transcription are indicated with *arrows*

Fig. 5 Scanning electron micrographs of *L. monocytogenes* mutant MN1 (**a**), EGD (**b**). *Bar* represents 2 μm
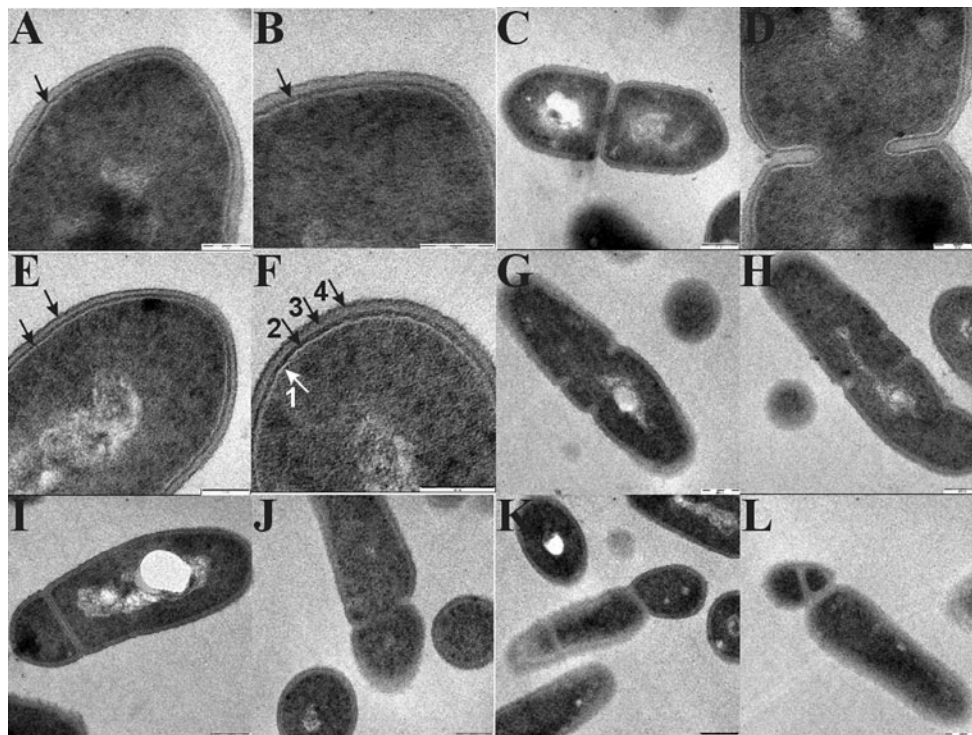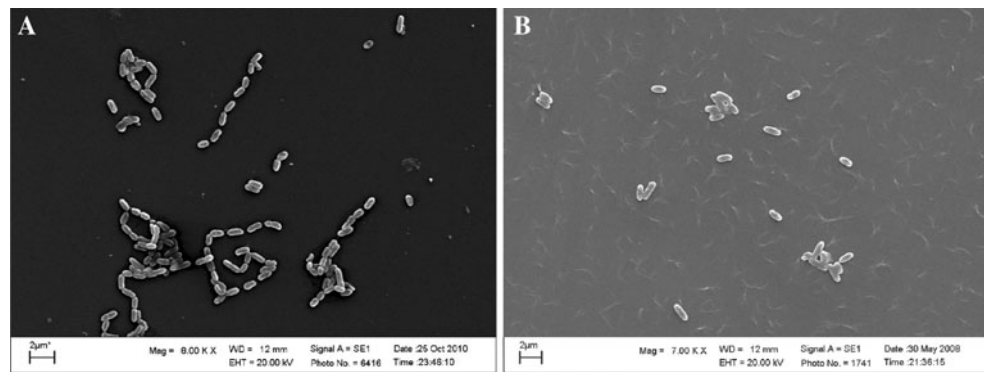

Fig. 6 Transmission electron micrographs of *L. monocytogenes* EGD (**a–d**) and mutant MN1 (**e–l**). *Bar* represents 100 nm (**a, b, d, e, f**) and 200 nm (**c, g, h, i, j, k, l**). At the bacterial wall region; (*1*) a low inner zone (*IWZ*) precedes (*2*) a high-density outer zone (*OWZ*); then (*3*) a fibrous layer and (*4*) the second high-density zone in bacterial wall of the MN1 cells. The plasma membrane resides immediately below the *IWZ* zone (according to Matias and Beveridge 2006)

to show abnormal cell division with a septum not at midcell but irregularly placed. Very often more than one septum was formed (Fig. 6g, h). During the process of cell division, a murein layer forming a new transverse septum is synthesized. The growth process of the cylindrical part of an existing bacterial cell wall consists of cutting bonds in the existing murein layer and insertion of new building murein subunits. In contrast, the creation of a transverse septum requires the intensive synthesis and construction of a new murein layer forming a double cell wall. It is not surprising, therefore, that such changes were observed during the growth and cell division of mutant cells with impaired peptidoglycan biosynthesis. The second point is

the reduction of TA in the cell wall of MN1 mutant cells. Very similar changes in cell morphology were observed by Dubail et al. (2006) in the case of a mutant of *L. monocytogenes* in lmo2537 gene encoding a UDP-GlcNAc 2-epimerase involved in TA biosynthesis. The authors concluded that the presence of TAs in the bacterial cell wall is required for both maintaining the shape of bacterial envelope and normal cell division.

Characterization of cell wall

The mutant strain exhibited clearly altered morphology with thinner and probably more cross-linked cell wall cells
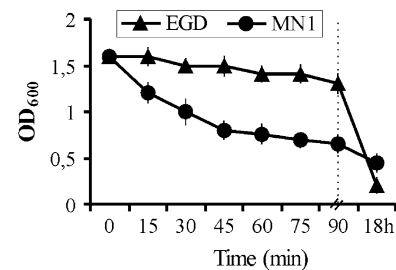
Table 4 Differences in the amount of murein, length of cells, and cell wall thickness of *L. monocytogenes* EGD and MN1 strain

EGD	MN1
CFU/ml (OD$_{600}$) of culture/weight of cells[a]	
CFU/ml (OD$_{600}$) of culture/weight of murein[b]	
1×10^9(1.713)/0.71 g = 2.41[a]	4×10^9(2.302)/0.72 g = 3.19[a]
1×10^9(1.713)/0.68 g = 2.52[b]	4×10^9(2.302)/0.70 g = 3.29[b]
Thickness of bacterial cell wall	
29.585 nm ± 2.134	22.712 nm ± 1.872
Length of bacterial cell	
0.734 μm ± 0.04	0.669 μm ± 0.03

Fig. 7 Sensitivity to mutanolysin. Bacteria were incubated with mutanolysin (in final concentration—29 μg/ml) at 37°C for 90 min. Lysis of bacterial cells was measured as a decline in optical density (OD$_{600}$) of the sample over time (at 15-min intervals for 90 min)

compared with the wild-type strain (Fig. 6a, b, e, f). This confirms our results obtained during the determination of relative OD$_{600}$ of culture/weight of cells or weight of murein when we found that to obtain the same weight in grams of cells or murein, four times more MN1 mutant cells needed to be taken compared to the wild-type strain EGD. A comparison of the murein content in the cell wall of the MN1 mutant revealed that it was about 60% of that of the parental EGD strain (Table 4). This points to a thinner cell wall of the mutant, which may also have a reduced amount of TAs, which are essential for maintaining cell shape and viability. In *B. subtilis* and *L. monocytogenes* the anionic wall TA increases the thickness of the outer wall zone (OWZ) either by extending from the surface and/or by expanding the peptidoglycan sacculus. Teichoic acids contribute to more than 40 or 70% of the dry weight of the *B. subtilis* or *L. monocytogenes* cell wall, respectively (Fujii et al. 1985; Rice and Bayles 2008).

In effect, the cells burst as a result of intracellular turgor when grown without osmoprotectants, as mentioned above, confirming the essential role of *lmo0956* in normal cell functioning and survival.

To assess the integrity of the cell wall, we tested the susceptibility of mutant MN1 to lysis after incubation with mutanolysin or with the antibiotics: peptide antibiotic, colistin; β-lactam, imipenem; tetracycline; glycopeptide, vancomycin; third-generation cephalosporin, ceftriaxone; aminoglycoside, gentamicin. *N*-acetylmuramidase and antibiotics that interfere with cell wall biosynthesis (imipenem, vancomycin, ceftriaxone) were used to confirm the

observed changes in both morphology and cell wall structure of the tested mutant. MN1 appeared to be more sensitive to the cell wall hydrolase (Fig. 7) than the wild strain EGD. The susceptibility of the mutant to antibiotics was evaluated on plates by disk diffusion method. The mutant showed an increased sensitivity toward colistin. After 48 h of incubation at 37°C an 8 mm diameter growth inhibition zone around the disk was observed. This was in contrast to EGD strain, for which no clearance zone was observed. The mutant showed slightly increased sensitivity to the other studied antibiotics (Table 5). A significant difference in zone diameter was found in the case of ceftriaxone (13 mm for EGD; 19 mm for MN1), which allows MN1, unlike the EGD, to be considered sensitive to this antibiotic (CLSI standards).

These results demonstrated that thinner bacterial cell wall and reduced quantities of the polymers covalently bound to the peptidoglycan (TAs) impaired cell wall integrity. A similar result was previously shown in a *dltA* mutant of *L. monocytogenes* lacking D-alanylation of LTA and TA (Abachin et al. 2002) and in *lmo2537* mutant encoding UDP-GlcNAc 2-epimerase of *L. monocytogenes* involved in TA biogenesis (Dubail et al. 2006). Since TA is covalently attached to peptidoglycan under conditions of reduced TA production the bacteria are likely to be more sensitive to drugs affecting the cell wall (colistin disrupts the phospholipid layer in cell membranes).

A reduced content of TA in the cell wall was found (confirmed) by determining the amount of phosphate present in the cell wall TA of the MN1 mutant and

Table 5 Susceptibility of *L. monocytogenes* EGD and MN1 mutant to select antibiotics

Strain of *L. monocytogenes*	Disk drug concentration (μg)/Diffusion zone breakpoint (mm)					
	Tetracycline [30 μg] (mm)	Vancomycin [30 μg] (mm)	Imipenem [10 μg] (mm)	Colistin [10 μg] (mm)	Ceftriaxone [30 μg] (mm)	Gentamicin [30 μg] (mm)
EGD	23	21	36	0	13	32
MN1	25	24	41	8	19	34

wild-type strains. The amount of cell wall phosphate in strain MN1 was significantly reduced to 0.75 μmol of phosphate per mg of cell wall, compared to 1.39 PO$_4$ per mg of EGD cell wall. This result is compatible with the involvement of the products of operon 150 genes (lmo0956, lmo0957, lmo0958) in biosynthetic amino-sugar precursor pathway required for cell wall peptidoglycan and TA biosynthesis. Most of the studies aimed at understanding the function of TA in gram-positive bacteria have been performed using *B. subtilis* strain 168 (Lazarevic et al. 2002). Mutations in all of the *tag* genes required for polyglycerol phosphate (TA) synthesis resulted in reduced cell wall phosphate content and in considerable changes in cell shape (Soldo et al. 2002a, b). It is interesting that when *B. subtilis* is grown under phosphate-limited conditions, the TAs are replaced by teichuronic acid. Teichuronic acid synthesis is dependent on the tua operon (*tuaABCDEFGH*) (Soldo et al. 1999). Bioinformatic analysis revealed no orthologous *tua* operon (BLAST) in the *Listeria* EGD genome.

Cryo-transmission electron microscopy (cryo-TEM) of frozen-hydrated sections of gram-positive bacteria allows visualization of the cell envelope in higher quality than other electron microscopy techniques that use chemical fixation and staining procedures. This technique reveals two different cell wall layers in gram-positive bacteria: an inner wall zone (IWZ) of low-electron density and an outer wall zone (OWZ) of high-electron density (Matias and Beveridge 2005, 2006). The IWZ has been suggested to be a region somehow analogous to the periplasmic space in gram-negative species (Matias and Beveridge 2005). The respiring cell produces a proton gradient outside of the cytoplasmic membrane that causes a localized reduction in the pH within the cell wall. This acidic pH suppresses the activity of murein hydrolases associated with the TAs and LTAs by promoting the protonation of the D-Ala ester linkages. Upon dissipation of the membrane potential, the pH in the cell wall increases and destabilizes or deprotonates the D-Ala ester linkages, thus derepressing the murein hydrolases. The OWZ contains peptidoglycan with covalently linked wall teichoic acid and cell surface proteins. It is obvious that the anionic wall teichoic acid increases the thickness of the OWZ, and therefore changes in the thickness of this layer are observed among gram-positive bacteria (Rice and Bayles 2008). Above the layer OWZ is the fibrous layer, suggested to be composed of partially degraded peptidoglycan on the outer surface of the cell wall, where peptidoglycan turnover is thought to take place. The thickness of the peptidoglycan layer of *Bacillus subtilis*, as detected by cryo-TEM, is 33.3 ± 4.7 nm in OWZ and 22.3 ± 4.8 nm in IWZ (Rice and Bayles 2008; Vollmer and Seligman 2010).

Transmission microscopic image analysis revealed also the possible existence of two layers of cross-linked murein

in the mutant cell wall in contrast to the wild-type strain cells, where it appears there is only one layer of highly cross-linked murein (Fig. 6). This layer is a fixed and unchanging part of the cell wall and is not subject to the process of turnover, in contrast to the murein layer located above it, which is subject to many changes associated with the process of growth and numerous modifications (Rice and Bayles 2008). For example, in the later stages of murein maturation (stationary phase of growth), numerous cross-links between peptide chains of murein are formed, resulting in increased cross-linking of murein (Vollmer and Seligman 2010). Because peptidoglycan biosynthesis in mutant cells is impaired, the murein is not able to grow normally.

To investigate whether there is any change in the muropeptides profile of murein, *N*-acetylated murein from wild-type and the mutant was prepared and analyzed by HPLC after digestion with the muramidase mutanolysin. The concentration of murein was 1 mg/ml and that of the muropeptides was in the range 0.2–0.5 mg/ml. The muropeptide profiles in the case of murein from both mutants were very similar to each other and different compared to the EGD profile. We identified 26 major peaks, 1–12 correspond to monomeric muropeptides, 13–22 correspond to dimeric muropeptides, 23 and over correspond to trimeric muropeptides. The decided reduction of several major peaks (nr 1, 4, 5, 6, 11, 12, 15, 16, 17, 20, 21, 22, 25, 26) in the case of the mutant murein is accompanied by an increase of five others (nr 8, 9, 18, 19, 23). Also, similar minor changes were observed (Fig. 8). In general, a decrease in all muropeptide fractions was observed (Table 6), but this was particularly evident for the main peaks in the fraction of monomeric muropeptides (4–6, 11);
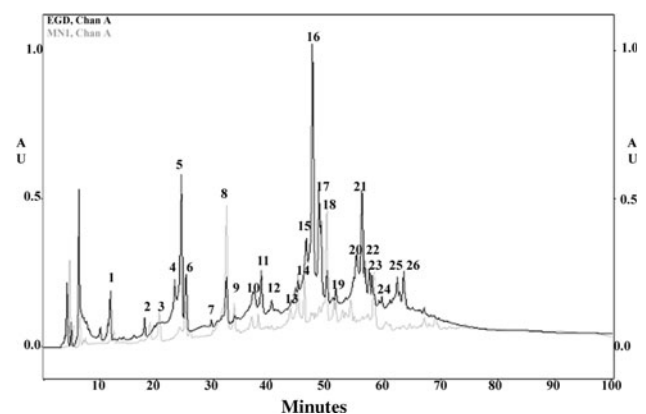

Fig. 8 HPLC analysis of the muropeptide composition of *L. monocytogenes* EGD and *nagA* mutant strains. HPLC elution patterns of muropeptides after digestion with mutanolysin of murein from *L. monocytogenes* (*black line*) and mutant MN1 (*gray line*). Peaks 1–12 correspond to monomeric muropeptides, 13–22 to dimeric muropeptides, and 23 and over to trimeric muropeptides

Table 6 Changes in muropeptide fractions in *L. monocytogenes* EGD and MN1 mutant

Muropeptide fraction	Sum of analyzed peak surface/muropeptide fraction (%)[a]		Ratio EGD/MN1
	EGD	MN1	
Monomers	29.957/20	24.676/14	1.214
Dimers	31.607/21	28.608/16.3	1.104
Trimers	5.047/3.3	4.489/2.5	1.124
Total	66.611/44.3	56.773/22.8	1.173

[a] Number of peaks analyzed is given in the legend to Fig. 8

smaller differences were observed in the fraction of dimeric muropeptides (15–17, 20–22) or in the fraction of trimeric muropeptides (23, 25, 26). Comparative analysis of the surface sum of the analyzed peaks showed a significant difference in the amount of highly cross-linked murein (oligomeric muropeptides), 55.7 for EGD versus 77.2 for MN1 (Table 6).

Conclusions

In this study it is reported that cytoplasmatic deacetylase (NagA) is essential for both maintaining the shape of the bacterial envelope and for normal cell division. The obtained results indicate the presence of two functional operons in *L. monocytogenes* cells, 150 carrying gene *lmo0956* and 348 carrying gene lmo2108. A detailed analysis of mutant MN1 demonstrated significant changes in the morphology of the bacterial cell and wall and in cross-linking of murein. Limited expression of *lmo0956* also reduced the amount of TA in the cell wall. This led to increased sensitivity to the peptidic antibiotic—colistin and to the third-generation cephalosporin—ceftriaxone, as well as to increased sensitivity to the cell wall hydrolase—mutanolysin. In addition, the participation of NagA-type enzyme in amino-sugar metabolism and a connection between amino-sugar metabolism pathways with cell wall peptidoglycan and teichoic acid biosynthesis has been proven. Because the mutant is unable to live in normal conditions, it will not be able to reproduce in either the environment or in host cells, which means it would not be effective in the process of infection/pathogenesis. Besides virulence, these proteins could have co-lateral effects on a number of important biological processes such as protein secretion or biofilm formation as observed with cell hydrolases Iap, Auto, or MurA (Desvaux et al. 2010; Renier et al. 2011). Therefore, the presented results point to the studied proteins as potential alternative targets for anti-listerial drug therapy.

References

Abachin E, Poyart C, Pellegrini E, Milohanic E, Fiedler F, Berche P, Trieu-Cuot P (2002) Formation of D-alanyl-lipoteichoic acid is required for adhesion and virulence of *Listeria monocytogenes*. Mol Microbiol 43:1–14

Ames BN (1966) Assay of inorganic phosphate, total phosphate, and phosphatases. Methods Enzymol 8:115–118

Arunkumar K, Manoj N (2010) Molecular evolution of the *N*-acetylglucosamine-6-phosphate deacetylase gene. In: ISB '10 Proceedings of the international symposium on biocomputing. ACM, New York. doi:10.1145/1722024.1722076

Barnhart MM, Lynem J, Chapman MR (2006) GlcNAc-6P levels modulate the expression of Curli fibers by *Escherichia coli*. J Bacteriol 188:5212–5219

Becker D, Selbach M, Rollenhagen C, Ballmaier M, Meyer TF, Mann M, Bumann D (2006) Robust *Salmonella* metabolism limits possibilities for new antimicrobials. Nature 440:303–307. doi:10.1038/nature04616

Boneca IG, Dussurget O, Cabanes D, Nahori MA, Sousa S, Lecuit M, Psylinakis E, Bouriotis V, Hugot JP, Giovannini M, Coyle A, Bertin J, Namane A, Rousselle JC, Cayet N, Prévost MC, Balloy V, Chignard M, Philpott DJ, Cossart P, Girardin SE (2007) A critical role for peptidoglycan *N*-deacetylation in *Listeria* evasion from the host innate immune system. Proc Natl Acad Sci USA 104:997–1002

Bouhss A, Trunkfield AE, Bugg TD, Mengin-Lecreulx D (2007) The biosynthesis of peptidoglycan lipid-linked intermediates. FEMS Microbiol Rev. Published article online, 07-Dec-2007

Boyd DA, Cvitkovitch DG, Bleiweis AS, Kiriukhin MY, Debabov DV, Neuhaus FC, Hamilton IR (2000) Defects in D-alanyl-lipoteichoic acid synthesis in *Streptococcus mutans* results in acid sensitivity. J Bacteriol 182:6055–6065

Chen PS, Toribara TY, Warner H (1956) Microdetermination of phosphorus. Anal Chem 18:1756–1758

Clemans DL, Kolenbrander PE, Debabov DV, Zhang Q, Lunsford RD, Sakone H, Whittaker CJ, Heaton MP, Neuhaus FC (1999) Insertional inactivation of genes responsible for the D-alanylation of lipoteichoic acid in *Streptococcus gordonii* DL1 (Challis) affects intrageneric coaggregations. Infect Immun 67:2464–2474

Collins LV, Kristian SA, Weidenmaier C, Faigle M, Van Kessel KP, Van Strijp JA, Gotz F, Neumeister B, Peschel A (2002) *Staphylococcus aureus* strains lacking ᴅ-alanine modifications of teichoic acids are highly susceptible to human neutrophil killing and are virulence attenuated in mice. J Infect Dis 186:214–219

Desvaux M, Dumas E, Chafsey I, Chambon C, Hébraud M (2010) Comprehensive appraisal of the extracellular proteins from a monoderm bacterium: theoretical and empirical exoproteomes of *Listeria monocytogenes* EGD-e by secretomics. J Proteome Res 9:5076–5092

Doyle RJ, Chaloupka J, Vinter V (1988) Turnover of cell walls in microorganisms. Microbiol Rev 52:554–567

Doyle RJ, Motley MA, Carstens PHB (1982) Turnover of cell wall in *Listeria monocytogenes*. Carbohydr Res 104:147–152

Dubail I, Bigot A, Lazarevic V, Soldo B, Euphrasie D, Dupuis M, Charbit A (2006) Identification of an essential gene of *Listeria monocytogenes* involved in teichoic acid biogenesis. J Bacteriol 188:6580–6591

European Committee on Antimicrobial Susceptibility Testing (2009) Antimicrobial susceptibility testing EUCAST disk diffusion method. Version 1.0. (www.eucast.org)

Fujii H, Kamisango K, Nagaoka M, Uchikawa K, Sekikawa I, Yamamoto K, Azuma I (1985) Structural study on teichoic acids of *Listeria monocytogenes* types 4a and 4d1. J Biochem 97:883–891

Glaser P, Frangeul L, Buchrieser C, Amend A, Baquero F, Berche P, Bloecker H, Brandt P, Chakraborty T, Charbit A, Chetouani F, Couve E, de Daruva A, Dehoux P, Domann E, Dominguez-Bernal G, Duchaud E, Durand L, Dussurget O, Entian K-D, Fsihi H, Garcia-Del Portillo F, Garrido P, Gautier L, Goebel W, Gomez-Lopez N, Hain T, Hauf J, Jackson D, Jones L-M, Karst U, Kreft J, Kuhn M, Kunst F, Kurapka G, Madueno E, Maitournam A, Mata Vicente J, Ng E, Nordsiek G, Novella de Pablos SB, Perez-Diaz J-C, Remmel B, Rose M, Rusniok C, Schlueter T, Simoes N, Tierrez A, Vazquez-Boland JA, Voss H, Wehland J, Cossart P (2001) Comparative genomics of *Listeria* species. Science 294:849–852

Glauner B (1988) Separation and quantification of muropeptides with high-performance liquid chromatography. Anal Biochem 172:451–464

Gross M, Cramton SE, Götz F, Peschel A (2001) Key role of teichoic acid net charge in *Staphylococcus aureus* colonization of artificial surfaces. Infect Immun 69:3423–3426

Hayashi H, Araki Y, Ito E (1973) Occurrence of glucosamine residues with free amino groups in cell wall peptidoglycan from bacilli as a factor responsible for resistance to lysozyme. J Bacteriol 113:592–598

Hughes AH, Hancock IC, Baddiley J (1973) The function of teichoic acids in cation control in bacterial membranes. Biochem J 132:83–93

Jaeger T, Mayer C (2007) *N*-acetylmuramic acid 6-phosphate lyases (MurNAc etherases): role in cell wall metabolism, distribution, structure, and mechanism. Cell Mol Life Sci 65:928–939

Jonquieres R, Bierne H, Fiedler F, Gounon P, Cossart P (1999) Interaction between the protein InlB of *Listeria monocytogenes* and lipoteichoic acid: a novel mechanism of protein association at the surface of gram-positive bacteria. Mol Microbiol 34:902–914

Joseph B, Goebel W (2007) Life of *Listeria monocytogenes* in the host cells' cytosol. Microbes Infect 9:1188–1195

Kovacs M, Halfmann A, Fedtke I, Heint M, Peschel A, Vollmer W, Hakenbeck R, Bruckner R (2006) Functional dlt operon, encoding proteins required for incorporation of D-alanine in teichoic acids in gram-positive bacteria, confers resistance to cationic antimicrobial peptides in *Streptococcus pneumoniae*. J Bacteriol 188:5797–5805

Lazarevic V, Abellan FX, Moller SB, Karamata D, Mauel C (2002) Comparison of ribitol and glycerol teichoic acid genes in *Bacillus subtilis* W23 and 168: identical function, similar divergent organization, but different regulation. Microbiology 148:815–824

Machata S, Hain T, Rohde M, Chakraborty T (2005) Simultaneous deficiency of both MurA and p60 proteins generates a rough phenotype in *Listeria monocytogenes*. J Bacteriol 187:8385–8394

Matias VR, Beveridge TJ (2005) Cryo-electron microscopy reveals native polymeric cell wall structure in *Bacillus subtilis* 168 and the existence of a periplasmic space. Mol Microbiol 56:240–251

Matias VR, Beveridge TJ (2006) Native cell wall organization shown by cryo-electron microscopy confirms the existence of a periplasmic space in *Staphylococcus aureus*. J Bacteriol 188:1011–1021

Mertins S, Joseph B, Goetz M, Ecke R, Seidel G, Sprehe M, Hillen W, Goebel W, Müller-Altrock S (2007) Interference of components of the phosphoenolpyruvate phosphotransferase system with the central virulence gene regulator PrfA of *Listeria monocytogenes*. J Bacteriol 189:473–490

Morath S, Geyer A, Hartung T (2001) Structure-function relationship of cytokine induction by lipoteichoic acid from *Staphylococcus aureus*. J Exp Med 193:393–397

Nouaille S, Commissaire J, Gratadoux JJ, Ravn P, Bolotin A, Gruss A, Le Loir Y, Langella P (2004) Influence of lipoteichoic acid D-alanylation on protein secretion in *Lactococcus lactis* as revealed by random mutagenesis. Appl Environ Microbiol 70:1600–1607

Park JT (2001) Identification of a dedicated recycling pathway for anhydro-*N*-acetylmuramic acid and *N*-acetylglucosamine derived from *Escherichia coli* cell wall murein. J Bacteriol 183:3842–3847

Park JT, Uehara T (2008) How bacteria consume their own exoskeletons (turnover and recycling of cell wall peptidoglycan). Microbiol Mol Biol Rev 72:211–227

Park SF, Stewart GS (1990) High-efficiency transformation of *Listeria monocytogenes* by electroporation of penicillin-treated cells. Gene 28:129–132

Peri KG, Goldie H, Waygood EB (1990) Cloning and characterization of the *N*-acetylglucosamine operon of *Escherichia coli*. Biochem Cell Biol 68:123–137

Peschel A, Otto M, Jack RW, Kalbacher H, Jung G, Götz F (1999) Inactivation of the dlt operon in *Staphylococcus aureus* confers sensitivity to defensins, protegrins, and other antimicrobial peptides. J Biol Chem 274:8405–8410

Peschel A, Vuong C, Otto M, Götz F (2000) The D-alanine residues of *Staphylococcus aureus* teichoic acids alter the susceptibility to vancomycin and the activity of autolytic enzymes. Antimicrob Agents Chemother 44:2845–2847

Piuri M, Sanchez-Rivas C, Ruzal SM (2005) Cell wall modifications during osmotic stress in *Lactobacillus casei*. J Appl Microbiol 98:84–95

Popowska M, Kusio M, Szymanska P, Markiewicz Z (2009) Inactivation of the wall-associated de-*N*-acetylase (PgdA) of *Listeria monocytogenes* results in greater susceptibility of the cells to induced autolysis. J Microbiol Biotechnol 19:932–945

Popowska M, Markiewicz Z (2006) Characterization of protein Lmo0327 of *Listeria monocytogenes* with murein hydrolase activity. Arch Microbiol 186:69–86

Porter KG, Feig YS (1980) The use of DAPI for identifying and counting aquatic microflora. Limnol Oceanogr 25:943–948

Ramaswamy V, Cresence VM, Rejitha JS, Lekshimi MU, Dharsana KS, Prasad SP, Vijila HM (2007) Listeria—review of epidemiology and pathogenesis. J Microbiol Immunol Infect 40:4–13

Renier S, Hébraud M, Desvaux M (2011) Molecular biology of surface colonization by *Listeria monocytogenes*: an additional facet of an opportunistic Gram-positive foodborne pathogen. Appl Environ Microbiol 13:835–850

Rice KC, Bayles KW (2008) Molecular control of bacterial death and lysis. Microbiol Mol Biol Rev 72:85–109

Sambrook J, Russel DW (2001) Molecular cloning. A laboratory manual. Cold Spring Harbor Laboratory Press, Cold Spring Harbor, New York

Schäferkordt S, Chakraborty T (1995) Vector plasmid for insertional mutagenesis and directional cloning in *Listeria* sp. Biotechniques 19:720–725

Schlech WF (2000) Epidemiology and clinical manifestation of *Listeria monocytogenes* infection. In: Fischetti VA, Novick RP, Ferretti JJ, Portnoy DA, Rood JI (eds), *Gram-positive pathogens*. ASM Press, Washington DC, American Society for Microbiology, p 473

Schwede T, Kopp J, Guex N, Peitsch MC (2003) SWISS-MODEL: an automated protein homology-modeling server. Nucl Acids Res 31:3381–3385

Scortti M, Monzó HJ, Lacharme-Lora L, Lewis DA, Vazquez-Boland JA (2007) The PrfA virulence regulon. Microbes Infect 9:1196–1207

Seveau S, Pizarro-Cerda J, Cossart P (2007) Molecular mechanisms exploited by *Listeria monocytogenes* during host cell invasion. Microbes Infect 9:1167–1175

Soldo B, Lazarevic V, Pagni M, Karamata D (1999) Teichuronic acid operon of *Bacillus subtilis* 168. Mol Microbiol 31:795–805

Soldo B, Lazarevic V, Karamata D (2002a) tagO is involved in the synthesis of all anionic cell-wall polymers in *Bacillus subtilis* 168. Microbiol 148:2079–2087

Soldo B, Lazarevic V, Pooley HM, Karamata D (2002b) Characterization of a *Bacillus subtilis* thermosensitive teichoic acid-deficient mutant: gene mnaA (yvyH) encodes the UDP-*N*-acetylglucosamine 2-epimerase. J Bacteriol 184:4316–4320

Szydłowska M, Markiewicz Z (1997) Convergence of the β-lactamase induction and murein recycling pathways in *Enterobacteria*. Acta Microbiol Pol 3:233–239

Toledo-Arana A, Dussurget O, Nikitas G, Sesto N, Guet-Revillet H, Balestrino D, Loh E, Gripenland J, Tiensuu T, Vaitkevicius K, Barthelemy M, Vergassola M, Nahori MA, Soubigou G, Régnault B, Coppée JY, Lecuit M, Johansson J, Cossart P (2009) The *Listeria* transcriptional landscape from saprophytism to virulence. Nature 459:950–956

Vincent F, Yates D, Garman E, Davies GJ, Brannigan JA (2004) The three-dimensional structure of the *N*-acetylglucosamine-6-phosphate deacetylase, NagA, from *Bacillus subtilis*: a member of the urease superfamily. J Biol Chem 279:2809–2816

Vollmer W (2007) Structural variation in the glycan strands of bacterial peptidoglycan. FEMS Microbiol Rev, Published article online, 07-Dec-2007

Vollmer W, Blant D, de Pedro MA (2008) Peptidoglycan structure and architecture. FEMS Microbiol Rev, Published article online, 08-Jan-2008

Vollmer W, Seligman SJ (2010) Architecture of peptidoglycan: more data and more models. Trends Microbiol 18:59–66

Vollmer W, Tomasz A (2000) The pgdA gene encodes for a peptidoglycan *N*-acetylglucosamine deacetylase in *Streptococcus pneumoniae*. J Biol Chem 275:20496–20501

Wecke J, Madela K, Fischer W (1997) The absence of D-alanine from lipoteichoic acid and wall teichoic acid alters surface charge, enhances autolysis and increases susceptibility to methicillin in *Bacillus subtilis*. Microbiol 143:2953–2960

Weidenmaier C, Kokai-Kun JF, Kristian SA, Chanturiya T, Kalbacher H, Gross M, Nicholson G, Neumeister B, Mond JJ, Peschel A (2004) Role of teichoic acids in *Staphylococcus aureus* nasal colonization, a major risk factor in nosocomial infections. Nat Med 10:243–245

Weidenmaier C, Peschel A (2008) Teichoic acids and related cell-wall glycopolymers in Gram-positive physiology and host interactions. Nat Rev Microbiol 6:276–287